# A COMPACT RF POWER COUPLER FOR THE NLC LINAC \*

G. Bowden<sup>†</sup>, W. B. Fowkes, R. J. Loewen, R. H. Miller, C. Ng, C. Pearson, J.W.Wang, SLAC, Stanford, CA

#### Abstract

A high power RF coupler connecting WR90 rectangular waveguide to the disc loaded waveguide accelerating structure of NLC is described. The coupler design is symmetric and free of beam deflecting field components. It makes an efficient electrical match between the rectangular waveguide power feed and the accelerator structure while keeping electrical surface field enhancement low. Electrical and mechanical design of the coupler are presented as well as quantitative comparisons between numerical simulation and low power cold test models.

## 1 DESIGN REQUIREMENTS AND EVOLUTION

One important component of any accelerating structure is the fundamental mode input coupler. It must provide a perfect match at the correct frequency between rectangular waveguide and the accelerating structure. To preserve low emittance in multi-bunch beams, rf field and phase must be made symmetric across the coupling cavity to avoid transverse deflections. To reduce manufacturing cost and improve mechanical stability, the design should be compact. Our previous coupler designs for NLC drove the coupling cavity through separate waveguides which were costly to manufacture and difficult to tune for perfect symmetric matching after assembly. The starting point for our present design was the DESY input coupler [1]. A set of initial dimensions for the coupling cavity and iris were based on previous NLC coupler designs. These were then adjusted during numerical simulations and later during cold test of prototype couplers.

### 2 MECHANICAL LAYOUT

Fig. 1 shows the coupler geometry with rf dimensions in mm for 11.424 GHz. The rf design was separated into an upper T branched WR90 rectangular waveguide and a lower symmetric side coupled accelerating cavity. The coupler is machined from a single block of copper (ASTM F-68 MET Class 2). A 10 mm thick cover plate is then hydrogen furnace brazed over the coupler front. To accommodate machining tolerances, the cavities' final rf impedance match will be adjusted by local deformation of cylindrical walls in the coupler and the following two cavities. Thin easily deformable regions in these walls will be created by drilling blind radial holes (not shown). Small stud screws will be brazed to the ends of these holes for pulling and

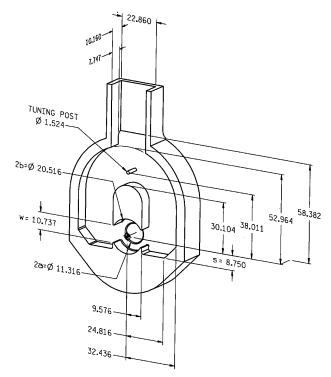


Figure 1: Input coupler geometry.

pushing so cavity resonant frequency can be both lowered as well as raised.

### 3 NUMERICAL SIMULATION

The matching and tuning of the compact RDDS<sup>1</sup> coupler structure is divided into two parts, namely, matching of the coupler cavity, and matching of the T-junction used for splitting the input power into two arms which feed the coupler cavity. The separation between the coupler cavity and T-junction is chosen long enough that effects of evanescent modes in connecting waveguides can be ignored. Thus overall matching can be achieved by matching each part individually.

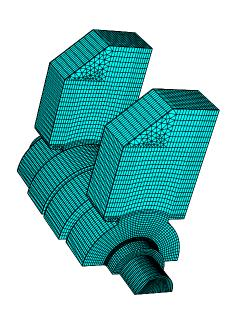
## 3.1 Matching and Tuning of the Coupler Cavity

The matching and tuning of the RDDS coupler is achieved by adjusting the coupler cell diameter 2b, the matching iris aperture w, and the terminated position of the waveguides s. (See Fig. 1.) The numerical procedure for achieving this has been studied previously [2]. Here, a new time-domain

 $<sup>^{\</sup>ast}\,\text{Work}$  supported by the Department of Energy, contract DE-AC0376SF00515.

<sup>†</sup> Email: gbb@SLAC.Stanford.EDU

<sup>&</sup>lt;sup>1</sup>RDDS stands for Round Damped Detuned Structure. The accelerating structure is a sequence of toroidal rounded cavities with dimensions chosen to detune higher order modes and damping slots to attenuate them.



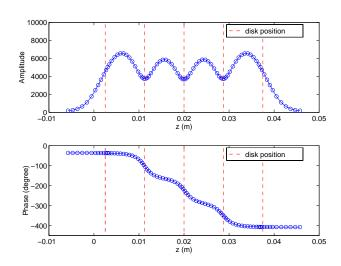


Figure 3: Longitudinal electric field along the axis

Figure 2: A 4-cell geometry for the coupler structure.

electromagnetic code, Tau3 [3], is employed for the numerical simulation. Tau3 uses an unstructured grid to model the exact curvatures of the structure. Fig. 2 shows the 3-dimensional model of the coupler structure using such an unstructured grid. The model consists of two coupler cells attached to identical input and output rectangular waveguides and two regular accelerator structure cells. Taking advantage of symmetry, only one half of the structure needs to be simulated. The transmission properties of the structure are determined by driving the  ${\rm TE}_{10}$  mode at the input rectangular waveguide. The reflection coefficient at the input waveguide and the transmission coefficient at the output waveguide are computed once steady state is reached.

The reflection coefficient for the matched coupler is found to be 0.005 at 11.424 GHz. The amplitude and phase of the longitudinal electric field along the axis for the matched coupler are shown in Fig. 3. Field gradient is about 15% higher in the coupler cell than in the structure cells. The phase changes in the coupler and regular cells are 60° and 120° respectively, indicating a traveling wave with the correct phase advance of 120° per cell from coupler to coupler.

## 3.2 Matching of T-junction

Figure 4 shows the 3-dimensional model of the T-junction used for Tau3 simulations. Again because of symmetry, only one half of the structure is simulated. The T-junction requires a post to improve the impedance match and a tran-

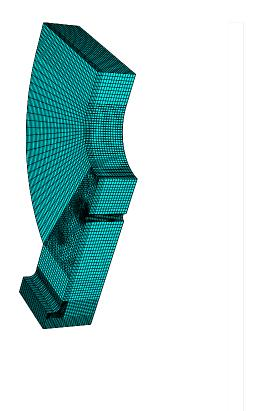


Figure 4: Geometry of the T-junction.

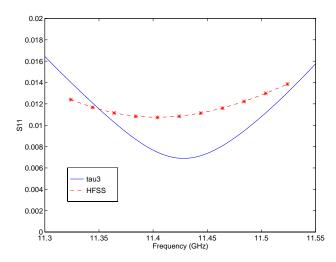


Figure 5:  $S_{11}$  spectrum of the T-junction.

sition step from the WR90 waveguide to the coupler thickness. The matching requirement of 0.01 reflection over a 200 MHz bandwidth centered at 11.424 GHz was met by adjusting the radii and locations of the post and step in the Tau3 simulation. Fig 5 shows that the reflection coefficient  $S_{11}$  at the WR90 input reaches a minimum of 0.007 at 11.424 GHz. Also plotted are the results of simulation using the HFSS code.

# 4 COUPLER COLD-TEST MEASUREMENTS

Final dimensions for the coupling iris w and cavity diameter 2b are determined by cold-testing. We start with a coupler assembly with excess metal (150 - 200  $\mu$ m) in both w and 2b. A stack of 15 traveling-wave cavities is clamped to the back of the coupler to provide a matching structure. A shorting plunger selectively detunes particular cells while a network analyzer measures the reflection coefficient. By iteratively machining, tuning the cell stack and remeasuring, an optimum set of dimensions is determined.

Kyhl's method [4] is used to evaluate coupling vs. tuning based on reflected phase at three frequencies calculated for the  $\pi/2$  mode and the desired  $2\pi/3$  modes. This method works reasonably well but an arbitrary reference of the coupler's shorting position and unknown calculational errors in the  $\pi/2$  mode frequency lead to some uncertainty. For this reason a time-domain measurement was also done as a cross check. A broadband display in the frequency domain provides the ability to analyze the effects of a short pulse of rf as it reflects off the coupler before interfering with the large mismatch at the end of the cell stack. Although this method cannot distinguish cell tunning mismatches from coupling mismatches, it provides a clear unambiguous measurement.

An important caveat to the time-domain procedure is the requirement that the cell stack is uniformly tuned. Inadvertent stagger tuning of the stack could cancel a coupler

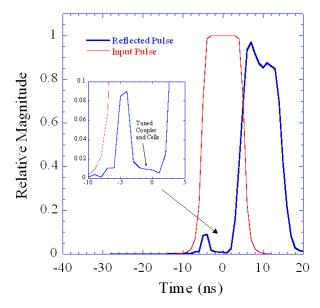


Figure 6: Coupler VSWR in the time domain.

mismatch. The RDDS structure has allowance for tuning only the first two cavities behind the coupler. Therefore as a final check, we randomly shuffled the cells in a tuned stack and verified the optimum coupler match by slight adjustment of the first two cavities. Fig. 6 illustrates the final time-domain measurement. After an initial reflection of high frequency components in the rise-time of the pulse, the coupler settles down to a VSWR of 1.02 before the end of the pulse is reached 8 ns later.

#### **5 REFERENCES**

- V. E. Kaljuzhny et. al., 'Design and Performance of a Symmetric High Power Coupler for a 6 Meter S-Band Linear Collider Accelerating Structure', DESY Internal Report DESY M-94-11, Oct. 1994, 32pp.
- [2] C.-K. Ng and K. Ko, Numerical simulation of input and output couplers for linear accelerator structures, Proc. CAP93, p243 (1993).
- [3] C.-K. Ng et. al., Simulation of RF structures in the time domain with unstructured grids, these proceedings.
- [4] E.P. Westbrook, 'Microwave Impedance Matching of Feed Waveguides to the Disk Loaded Accelerator Structure Operating in the 2Pi/3 Mode', SLAC-TN-63-103, Dec 1963. 18pp.